J Membrane Biol (2013) 246:151–160
DOI 10.1007/s00232-012-9515-6

A Theoretical Study of Single-Cell Electroporation in a Microchannel

Saeid Movahed · Dongqing Li

Received: 4 July 2012 / Accepted: 15 October 2012 / Published online: 6 November 2012

Abstract Electroporation of a single cell in a microchannel was studied. The effects of electrical (e.g., strength of the electric pulse) and geometrical (e.g., microchannel height, electrode size and position) parameters on cell membrane permeabilization were investigated. The electrodes were assumed to be embedded in the walls of the microchannel; the cell was suspended between these two electrodes. By keeping the electric pulse constant, increasing the microchannel height reduces the number and the radius of the biggest nanopores, as well as the electroporated area of the cell membrane. If the width of the electrodes is bigger than the cell diameter, the transmembrane potential will be centralized and have a sinusoidal distribution around the cell if nanopores are not generated. As the width of the electrode decreases and becomes smaller than the cell diameter, the local transmembrane potential decreases; in the nonelectroporative area, the transmembrane potential distribution deviates from the sinusoidal behavior; the induced transmembrane potential also concentrates around the poles of the cell membrane (the nearest points of the cell membrane to the electrodes). During cell membrane permeabilization, the biggest nanopores are initially created at the poles and then the nanopore population expands toward the equator. The number of the created nanopores reaches its maximal value within a few microseconds; further presence of the electric pulse may not influence the number and location of the created nanopores anymore but will develop the generated nanopores. Strengthening the electric pulse intensifies the size and number of the created nanopores as well as the electroporated area on the cell membrane.

Keywords Microchannel · Cell · Membrane · Electroporation · Electropermeabilization

S. Movahed · D. Li (✉)
Department of Mechanical and Mechatronics Engineering, University of Waterloo, Waterloo, ON N2L 3G1, Canada
e-mail: dongqing@mme.uwaterloo.ca

Introduction

The presence of an external electric field near the cell membrane may have different effects, ranging from manipulating the cell (Gimsa 2001; Yuejun and Li 2009) to altering the cell membrane structure (Wong et al. 2005; Movahed and Li 2011a). When the cell membrane is in contact with aqueous solutions, ionization of the surface molecules or absorption of the ions from the liquid solution causes electric charge on the cell membrane. Previous studies have revealed that cells start growing in the presence of an externally applied electric field under certain ranges of electric field intensity and duration (Wang et al. 2006). Electroporation is one of the most interesting influences of the electric field on the cell membrane. Applying an electric pulse near the cell alters the electric potential difference on both sides of the cell membrane; this difference is usually termed the *transmembrane potential* (TMP). When the applied electric field is larger than a critical TMP value, the cell membrane structure will be disturbed significantly and nanopores are created in the cell membrane. This leads to a significant increase in the electrical conductivity and permeability of the cell, referred to as electroporation or electropermeabilization (Krassowska and Neu 2009; Weaver 1995). Electroporation has many applications in biomedical treatment such as gene therapy (Valero et al. 2008; Zhengzheng et al. 2007; Li 2008b), electrochemotherapy (Gothelf et al. 2003), electrogenetransfection (Valero et al. 2008), electrofusion (Cao

et al. 2008; Schaper et al. 2007), transdermal drug delivery (Herwadkar and Banga 2012), cell lysis (Lin and Leea 2009), and cell transfection (Wang et al. 2009). In many of these applications, the cells should remain viable after electroporation. Thus, the electric pulse duration and intensity should be controlled precisely in order to not cause permanent effects on the cell structure or kill the cells.

Many experimental studies on cell electroporation have been conducted (Wang et al. 2010; Fox et al. 2006; Movahed and Li 2011b; Lee et al. 2009; Shik et al. 2004). The idea of performing cell electroporation in microfluidic systems has been pursued since the beginning of this millennium (Huang and Rubinsky 2000, 2001, 2003). Recent developments of biomedical microfluidic devices tempt more and more researchers to use these instruments for cell studies (Jiang et al. 2011; Bao et al. 2010). Microfluidic devices offer many advantages such as a significant reduction in consumption of reagents. Furthermore, they provide the feasibility of performing single-cell studies. Previous studies have revealed that, in comparison with traditional electroporative systems, performing single-cell electroporation in microfluidic systems substantially improves cell viability and the transfection rate of biological samples into the cells (Lee et al. 2009).

So far, theoretical studies on cell electroporation have lagged behind experimental ones, though they are completely essential to boost the current understanding of the mechanism of cell electroporation, reduce the side effects of the external electric field on the cell structure and increase electroporation efficiency. The current theoretical studies on cell electroporation can be categorized into three main classes. The first group includes the studies that investigate the effects of different parameters such as field strength, ionic concentration, pulse strength and duration on cell permeabilization (Li and Lin 2011; DeBruin and Krassowska 1999a, b; Talele et al. 2010; Bilska et al. 2000). The second category focuses on optimizing and control of the electric pulse during cell electroporation (Zhao et al. 2010; Miklavcic and Towhidi 2010). The third set evaluates the uptake of fluid, ions and macromolecules by the cell during electroporation (Zaharoff et al. 2008; Granot and Rubinsky 2008; Movahed and Li 2012; Li and Lin 2011). Once the radius and location of the created nanopores are calculated, different models can be utilized to find the mass transfer through these nanoscale pores (Movahed and Li 2011a; Zangle et al. 2010; Rafiei et al. 2012).

In a series of articles, DeBruin and Krassowska studied the effect of field strength, rest potential and ionic concentration on cell permeabilization (DeBruin and Krassowska 1999a, b). They found that the TMP (the difference of the electric potential on the two sides of the cell membrane) is symmetric about the equator, with the same value at both poles of the cell. As the nanopores are created, increasing the electric field intensity does not affect the maximum magnitude of TMP; however, this will create more nanopores on the cell membrane and increase the electroporated area of the cell membrane. They also showed that TMP is independent of rest potential (the electric potential inside the cell when it is not stimulated by the external electric field). In 2007, Krassowska and Filev (2007) investigated the pore density around the cell. According to their results, the highest pore density occurs on the depolarized pole (the nearest point on the cell membrane to the negative electrode) and the hyperpolarized pole (the nearest point on the cell membrane to the positive electrode), but the largest pores are on the border of the electroporated regions of the cell. Despite their much smaller number, large pores comprise 95.3 % of the total pore area and contribute 66 % to the increased cell conductance. In 2010, Talele et al. (2010) developed a numerical model for single- and spherical cell electroporation. They simulated spatial and temporal aspects of the TMP and pore radii as an effect of applied electric field. Based on their results, the pore radii tend to be uniform for AC fields. The relative difference in electroporated area is reduced by the use of a 1-MHz sinusoidal applied electric field over a 100-kHz field.

The effect of electric pulse shape on the electroporation efficiency is important. Different pulse shapes can generate various effects on the cell (Fox et al. 2006). In 2010 Miklavcic and Towhidi (2010) proposed an analytical model to predict the effects of arbitrarily shaped electroporation pulses on cell membrane conductivity and molecular transport across the cell membrane. Some studies used feedback control techniques to reduce the side effects of the electric pulse on the cell structure. One of the first analytical studies on closed-loop control of cell electroporation was conducted on 2010 by Zhao et al. (2010). Using a nonlinear control technique, they regulated the input voltage to stabilize the generated pore radii around the desired value. Several studies were also conducted on the mass transfer and uptake rate into the cells during electroporation (Movahed and Li 2012; Li and Lin 2011). As an example, Li and Lin (2011) solved mass transfer equations to find the insertion of calcium ions into a Chinese hamster via these created nanopores.

It should be pointed out that all the reported studies on cell membrane permeabilization (creating nanopores on the cell membrane due to applied electric field) considered the cells in an infinitely large medium. In microfluidic devices, the cells are usually located in microchannels or microchambers. The results of the current published studies may not reflect the boundary effects of microfluid-based electroporative devices. Moreover, the size and position of electrodes may have significant influences on membrane

permeabilization. In this study, we investigated the membrane permeabilization of a single cell located in a straight microchannel. The pulse shape was chosen as a square wave, which is widely used in the microfluidic devices (Wang and Lu 2006a, b; Wang et al. 2006; Ionescu-Zanetti et al. 2008; Wang and Lu 2006a; Khine et al. 2005; Vassanelli et al. 2008). This electric pulse shape can be easily generated by contracting the cross-sectional area of the microchannels or using a high-voltage pulse generator. We studied the effects of microchannel height, electrode dimensions, pulse intensity and duration on the distribution and radius of the created nanopores on the cell membrane. The rest of this article is organized as follows. The following section explains the model considered in the current study. The mathematical modeling and governing equations of cell membrane permeabilization are introduced (see "Numerical Simulation"). The Results and Discussion section describes the numerical approach of the current study.

Model Description

Figure 1 shows a schematic diagram of the system in the current study. A spherical cell of radius a (diameter d_0) immersed in a microchannel of height h_c is considered. The microchannel is filled with a conductive medium (an aqueous solution). The thickness of the cell membrane is assumed to be h. The required electric pulse for electroporation (ϕ_0) is applied to the cell via the two electrodes on the side walls of the microchannel. Five points are defined on the cell membrane: D and H are the depolarized (DP) and hyperpolarized (HP) poles, E indicates the equator line and D_b and H_b define the border between the electroporated and the nonelectroporated regions on the membrane. The values of these parameters used in the current study are listed in Table 1.

In the theory of cell membrane permeabilization, there are two kinds of pores in the cell membrane: hydrophobic and hydrophilic. Hydrophobic pores are gaps in the lipid bilayer of the membrane that are formed by thermal fluctuation. Hydrophilic pores have their walls lined with the water-attracting heads of lipid molecules. Different from hydrophobic pores, hydrophilic pores allow the transport of water-soluble substances, such as ions, and thus conduct electric current. In this study, we investigated the creation of hydrophilic nanopores in the presence of an applied electric field. When the TMP reaches values of 0.5–1 V, hydrophilic nanopores will be created with an initial radius of r^*. In fact, r^* is the threshold radius where hydrophobic nanopores convert to hydrophilic ones. In the current study, we applied the asymptotic ODE model (Neu and Krassowska 1999) to the system shown in Fig. 1 to investigate cell membrane permeabilization in a microchannel. In previous studies, the energy concept was utilized to develop a mathematical model of cell membrane permeabilization in terms of a set of partial differential equations (PDEs) (Neu and Krassowska 1999). It is difficult to solve this set of PDEs numerically because of the presence of disparate spatial and temporal scales. In Ref. (Neu and Krassowska 1999), the authors proposed an asymptotic reduction of the PDE to an ordinary differential equation

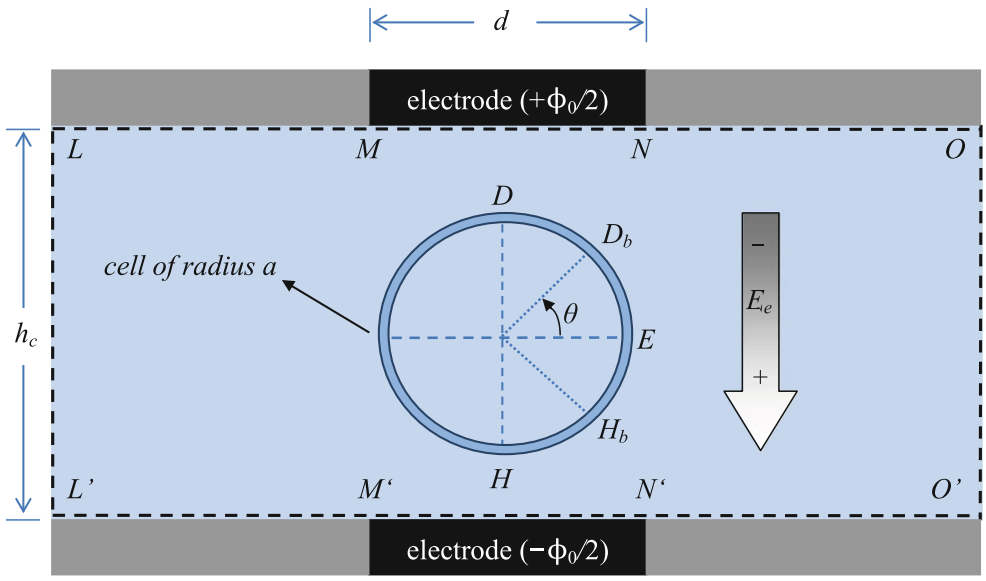

Fig. 1 Schematic diagram of the assumed system of the current study. A cell of radius a is assumed in the microchannel of height h_c. The microchannel is filled with the conductive medium. The required voltage of the electroporation (ϕ_0) is applied via the two electrodes of length d located on the wall of the microchannel

Table 1 Values for constants and parameters used in the simulations

Parameter	Value/range	Unit
a	15	μm
h	5	nm
h_c	20–30	μm
d	10–20	μm
ϕ_0	1–3	V
t_0	10–20	μs
s_i	0.455	S m^{-1}
s_e	5	S m^{-1}
s	2	S m^{-1}
c_m	0.0095	F m^{-2}
g_1	2	S m^{-2}
V_{rest}	−80	mV
α	1×10^9	m^{-2}s^{-1}
V_{ep}	0.258	V
N_0	1×10^9	m^{-2}
r^*	0.51	nm
D	5×10^{-14}	m^2 s^{-1}
k	1.38065×10^{-23}	m^2 kg s^{-2} K^{-1}
T	300	K
β	1.4×10^{-19}	J
γ	1.8×10^{-11}	J m^{-1}
$F_{\max}$	0.7×10^{-9}	N V^{-2}
r_h	0.97×10^{-9}	m
r_t	0.31×10^{-9}	m
q	$(r_m/r^*)^2$	–
σ'	2×10^{-2}	J m^{-2}
σ_0	1×10^{-6}	J m^{-2}

ODE, which is easier to solve by numerical methods. Further information about this approach can be found in Ref. (Neu and Krassowska 1999). In the present study, we applied this ODE model to the cell located in the microchannel to study the effects of various boundary conditions, including the microchannel dimensions and the location and size of the electrodes on cell membrane permeabilization.

Electric Field

The Laplace equation should be solved to find the electric potential inside (ϕ_i) and outside (ϕ_e) the cell.

$$\nabla^2 \phi_{i,e} = 0 \tag{1}$$

The required voltage of electroporation (ϕ_0) is applied via the embedded electrodes on the two sides of the cells. Thus, the electrical boundary condition on boundaries MN and $M'N'$ is assumed as

$$\phi_{e,MN} = \phi_0/2 \tag{2a}$$

$$\phi_{e,M'N'} = -\phi_0/2 \tag{2b}$$

The walls of the microchannels are electrically insulated. There is also no current flow at the two ends of the microchannel. Therefore, the assumed electrical condition on boundaries LM, NO, OO', $O'N'$, $M'L'$ and $L'L$ is

$$\hat{n} \cdot \vec{J} = 0 \tag{3}$$

The electric current density should be continuous across the cell membrane:

$$\begin{aligned} -\hat{n} \cdot (s_i \nabla \phi_i) &= -\hat{n} \cdot (s_e \nabla \phi_e) \\ &= c_m \frac{\partial V_m}{\partial t} + g_1 (V_m - V_{\text{rest}}) + I_p \end{aligned} \tag{4}$$

In this equation $\hat{n}$ is the local outward unit vector normal to the surface of cell membrane, ∇ is the Nabla symbol, s_i and s_e are the interacellular and extracellular conductivities, V_m and V_{rest} are the TMP and rest potential and g_1 and c_m are the surface conductance and capacitance of the membrane, in that order.

The TMP (V_m) is defined as

$$V_m = \phi_i(t, a, \theta) - \phi_e(t, a, \theta) \tag{5}$$

The first and second terms of the right-hand side of Eq. 4 represent the capacitive current ($c_m \partial V_m/\partial t$) and the current through the protein channels ($g_1(V_m - V_{\text{rest}})$), respectively. I_p represents the current through the created nanopores. If the cell membrane is discretized into k elements, the surface area of each segment can be found as $\Delta A = 2\pi a/k$. At each of these sections of membrane, I_p can be found as

$$I_p(t) = \frac{1}{\Delta A} \sum_{j=1}^{m} i_p(r_j, V_m) \tag{6}$$

Here, m is the number of created nanopores at each segment and i_p is the current through each nanopore, which can be computed using the following equation:

$$i_p(r, V_m) = \frac{V_m}{R_p + R_i} \tag{7}$$

where R_p is the ohmic resistance of the cylindrical pores and R_i is the correcting resistance that is used to consider the effect of changing TMP in the vicinity of the pores.

$$R_p = \frac{h}{s\pi r^2} \tag{8}$$

$$R_i = \frac{1}{2sr} \tag{9}$$

In the above equations, h and s are the membrane thickness and conductivity of the solution filling the nanopore, respectively.

Number of Nanopores

The rate of creation of nanopores can be found as

$$\frac{dN(t)}{dt} = \alpha e^{(V_m/V_{ep})^2}\left(1 - \frac{N(t)}{N_{eq}(V_m)}\right) \tag{10}$$

where $N(t)$ is the density of pores, defined as

$$N(t) = \int_{r*}^{\infty} n(r,t)dr \tag{11}$$

N_{eq} is the equilibrium pore density for the given transmembrane voltage, V_m:

$$N_{eq}(V_m) = N_0 e^{q(V_m/V_{ep})^2} \tag{12}$$

In the above equations, α, V_{ep}, q and N_0 are the constants that can be found in Table 1.

Radius of Nanopores

Based on the theory of membrane permeabilization, nanopores are initially created with a radius of $r*$. By increasing the applied electric field, nanopores start to develop in order to minimize the energy of the cell membrane. For the membrane with n nanopores, the rate of change of their radii, r_j, can be determined by the following set of equations:

$$\frac{dr_j}{dt} = U(r_j, V_m, \sigma_{eff}), \quad j = 1, 2, \ldots, n \tag{13a}$$

$$U(r, V_m, A_p) = \frac{D}{kT}\left\{4\beta\left(\frac{r*}{r}\right)^4\frac{1}{r} - 2\pi\gamma + 2\pi\sigma_{eff}r + \frac{V_m^2 F_{Max}}{1 + r_h/(r + r_t)}\right\}, \quad \text{in } r \geq r* \tag{13b}$$

The constants of the above equations are defined in Table 1. σ_{eff} is the effective tension of the membrane. If A is the surface area of the cell membrane and A_p is the area of the created nanopores ($A_p = \sum_{i=1}^{n}\pi r_i^2$), σ_{eff} can be computed as

$$\sigma_{eff}(A_p) = 2\sigma' - \frac{2\sigma' - \sigma_0}{\left(1 - A_p/A\right)^2} \tag{14}$$

Numerical Simulation

In this study, Eqs. 1–14 were solved numerically to find the electric potential in the domain and to investigate the creation of nanopores on the cell membrane. The Comsol 3.5a (http://www.comsol.com/) commercial package was used in the numerical simulations. The cell membrane was discretized with a discretization step of $\Delta\theta = \pi/60$. In order to discretize the solution domain, unstructured meshes were applied. The solution domain was broken into small meshes to allow meshes to fully cover the solution domain without overlapping.

Before applying the electric pulse, TMP was equal to the rest potential ($V_m = V_{rest}$). At each time step, Eqs. 1–5 were solved by the finite element method to find the electric potential in the domain. After the electric potential was obtained, Eqs. 6–14 were solved to find the location, number and radius of the created nanopores on the membrane. The Runge–Kutta method was utilized to solve ODE Eqs. 10 and 13a. This system of equations was solved with a time step of $\tau_c/32$, in which τ_c is the time constant of the cellular polarization (Hibino et al. 1993):

$$\tau_c = aC_m\left(\frac{1}{s_i} + \frac{1}{s_e}\right) = 2.4\,\mu s \tag{15}$$

Results and Discussion

The quantitative information used in the simulations is provided in Table 1. A cell of radius a (15 μm) is considered in the microchannel of height h_c (25–35 μm). The necessary electric field (1–3 V) was applied by the two electrodes of width d (5–20 μm) located on the walls of the microchannel. The electric pulse span was on the order of microseconds. In this section, we present the influence of electric pulse intensity (ϕ_0) and duration (t_0),electrode size (d) and microchannel height (h) on the electropermeabilization of the cell. The pulse shape was chosen as a square wave and can be mathematically expressed as $V = \phi_0 \times u(t–t_0)$. Here, $u(t–t_0)$ is the step unit function that is equal to one for $0 \leq t \leq t_0$ and zero for $t > t_0$ (see Fig. 2).

The results show that nanopore radius and density are symmetric along the equator (see Fig. 1). The TMP has the same magnitude with the opposite sign on the two sides of the cell membrane ($0° \leq \theta \leq 180°$ and $180° \leq \theta \leq 360°$). Therefore, in the present study, only the permeabilization of the back side of the cell membrane has been illustrated ($180° \leq \theta \leq 360°$).

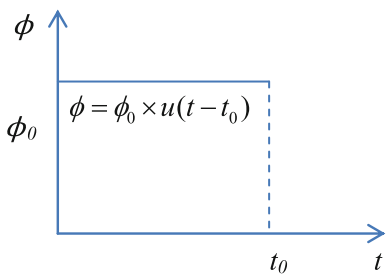

Fig. 2 Schematic diagram of the applied electric pulse

Time Evaluation

For one specific case (h_c = 30 μm, a = 15 μm, ϕ_0 = 3 V and d = 20 μm), Fig. 3 depicts the TMP and the radius of the generated nanopores on the back side of the cell membrane. Once the nanopores are generated, the TMP reduces. The TMP has a sharper reduction at the poles ($\theta = 90°$ and 270°). At the beginning ($t \leq 2$ μs), the biggest nanopores are created at *DP* and *HP* poles. As the nanopores are created, TMP decreases and the angular positions of the highest TMP and the biggest nanopores move toward the equator (*E*). For this case, Fig. 4 depicts the density of the created nanopores (*N*). This figure shows that the number of generated nanopores reaches its maximum value very fast (1–2 μs). From the results shown in Figs. 3 and 4, once the nanopores are created, their number and location may not be influenced by the electric pulse anymore; the electroporated area also remains unchanged. Further presence of the electric pulse results in developing the size of the generated nanopores. Here, the energy level of the cell membrane increases in the presence of the electric pulse. According to the theory of membrane permeabilization, the created nanopores consume the absorbed energy in order to keep growing, resulting in reduction in the TMP. The numerical results of this study also agree with this fact (see Figs. 3, 4).

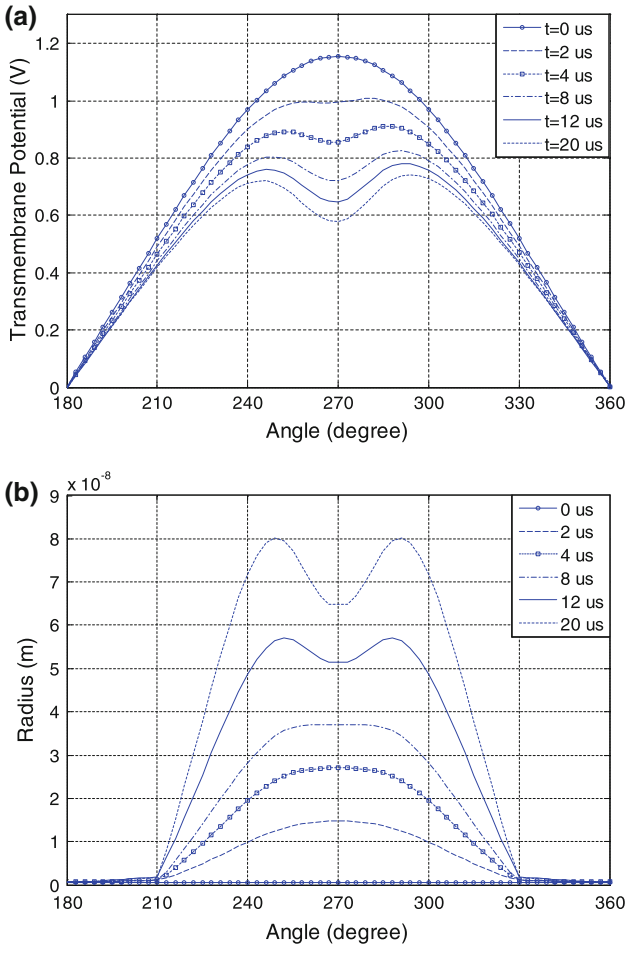

Fig. 3 Time evaluation of the membrane permeabilization of a cell located in the microchannel (h_c = 30 μm, a = 15 μm, ϕ_0 = 3 V, and d = 20 μm). **a** Transmembrane potential. **b** Radius of the created nanopores

Electrode Size

Figure 5 illustrates the effect of electrode size (d) on the TMP before the nanopores are created on the cell membrane. A parameter x is defined as the ratio of the electrode width (d) to the cell diameter (d_0), i.e., $x = d/d_0$.

For cells located in an infinite domain and exposed to a uniform electric field of E_e, if the nanopores are not created, the TMP is given by the Schuwan equation (Pauly and Schwan 1959):

$$V_m = 1.5E_e a\cos(\theta) \tag{16}$$

The Schuwan equation shows that in an infinite domain, if the nanopores are not created on the cell membrane, TMP has a sinusoidal distribution. For the cell located in a microchannel as shown in Fig. 1, the numerical simulation also shows that TMP has a sinusoidal profile around the cell membrane when $x > 1$. However, as the ratio of the electrode width to the diameter of the cell decreases, the following occurs (see Fig. 5): (1) the local TMP value reduces and (2) TMP values decrease sharply from the poles of the cell membrane ($\theta = 90°$ and 270°) to the equator ($\theta = 0°$ and 180°).

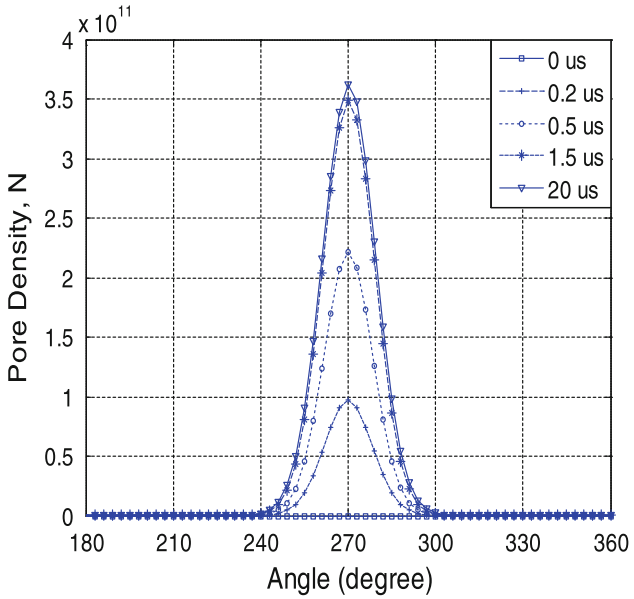

Fig. 4 Time evaluation of the density of the created nanopores on the membrane of the cell located in the microchannel. (h_c = 30 μm, a = 15 μm, ϕ_0 = 3 V, and d = 20 μm)

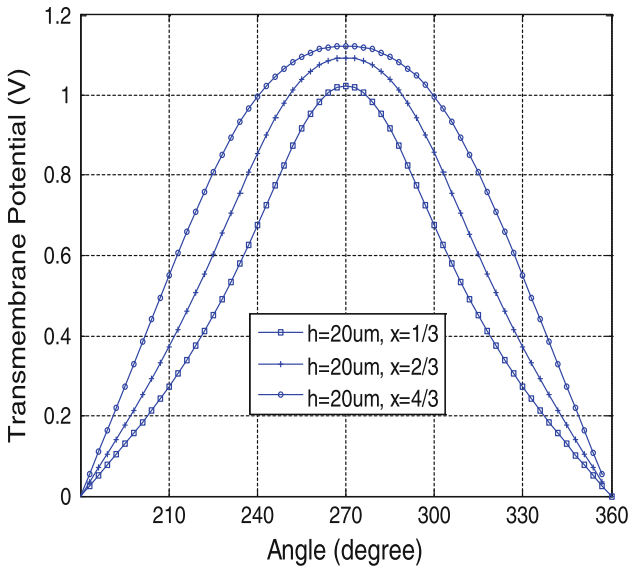

Fig. 5 Illustration of the effect of electrode size on transmembrane potential before nanopores are created. The parameter is defined as the ratio of electrode width (d) to the cell diameter (d_0), i.e., $x = d/d_0$ ($a = 15$ μm, $\phi_0 = 2.3$ V)

If the applied voltage is kept constant, decreasing the height of the microchannel (the distance between the two electrodes) produces a stronger electric field; consequently, the local TMP will be increased and nanopores are created with a smaller applied voltage via the electrodes. Figure 5 also depicts the effect of electrode size on the initial TMP; here, the nanopores have not been created yet. Larger values of the initial TMP will produce more nanopores on the cell membrane. The TMP tends to decrease less sharply for higher values of x. Therefore, increasing the width of the electrodes enhances the local TMP on the cell membrane. Hence, if we aim to increase the created nanopores on the cell membrane, the width of the electrode should be larger than the cell diameter (useful in transfection applications). Thus, in order to maximize the efficiency of cell transfection (reversibly electroporate the cell to insert biological samples into the cell), the width of the electrode should be bigger that the cell diameter. If the interest is to electroporate only a specific part of the cell (e.g., in electrofusion), x may be smaller than 1.

Microchannel Height and Pulse Intensity

Figures 6 and 7 illustrate the effects of microchannel height (h_c) and pulse intensity (ϕ_0) on the permeabilization of the cell membrane. In these figures, the microchannel heights are 25, 30 and 35 μm. The applied electric pulse intensities are 1, 1.5, 2 and 2.3 V. The pulse span is kept constant ($t_0 = 10$ μs).

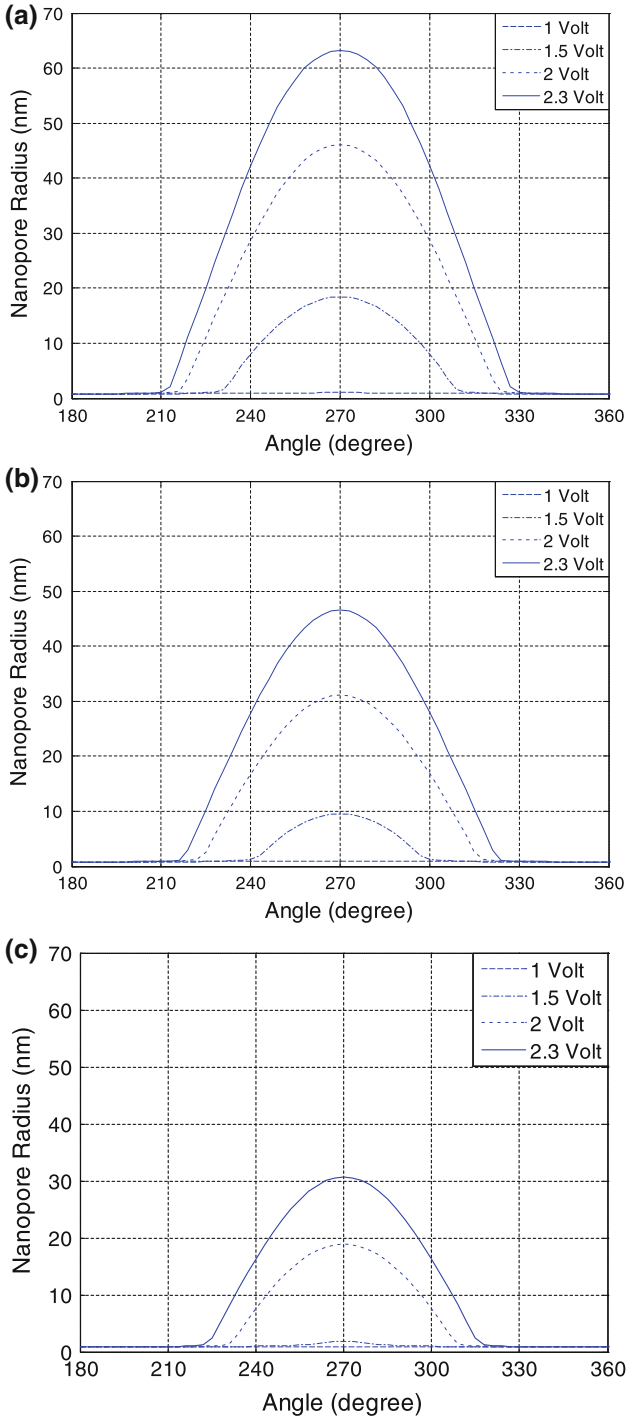

Fig. 6 Effect of pulse intensity on the radius of the created nanopores on a cell of diameter 15 μm. Heights of microchannels are 25 μm (**a**), 30 μm (**b**) and 35 μm (**c**)

As seen in these figures, both electric pulse intensity and microchannel height have great influence on the radius and density of the created nanopores. For the same-size microchannels, intensifying the electric pulse increases both the density and the radius of the created nanopores. As an example, Figs. 6a and 7a show that for $h_c = 25$ μm,

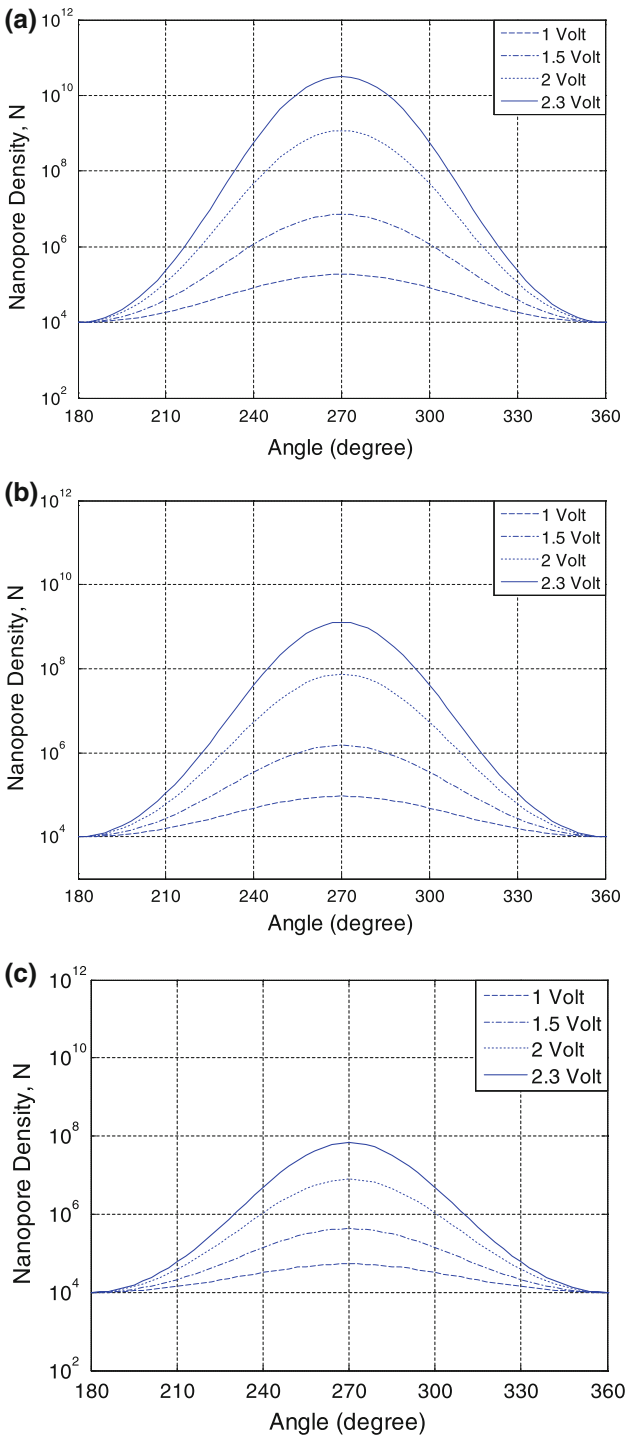

Fig. 7 Effect of pulse intensity on the density of created nanopores on a cell of diameter 15 μm. Assumed heights of microchannels are 25 μm (**a**), 30 μm (**b**) and 35 μm (**c**)

when the applied electric pulse is $\phi_0 = 1$ V, the generated nanopore size is minimal. By increasing the applied electric pulse from 1 to 2 V, the maximum radius of the nanopores reaches ~45 nm. If the applied electric pulse is enhanced to 2.3 V, the maximum radius of the nanopores reaches ~65 nm. These maximum-size nanopores are mainly located around the poles ($\theta = 270°$) (Fig. 7). Intensifying the electric pulse also expands the electroporated area of the cell membrane. For example, consider the case of a microchannel height of 25 μm (Figs. 6a, 7a). When the applied voltage is 1 V, no significant nanopores are created on the cell membrane. However, when the applied voltage increases to 1.5 and 2 V, the angular area with a significant number of electroporated nanopores covers approximately $230° \leq \theta \leq 310°$ and $215° \leq \theta \leq 325°$, respectively (see Fig. 7a).

Conclusion

In this study, membrane permeabilization of a single cell in a microchannel was investigated. The previous studies on cell electroporation consider cells in an infinite domain, which does not reflect the finite boundary effects of microchannel walls on the membrane permeabilization process. In our study, we found that the size of the microchannels and electrodes as well as the position of the electrodes in the microchannels have a great influence on cell electroporation.

The following conclusions have been drawn:

- In microfluidic electroporative devices, membrane permeabilization can be performed with very low-intensity electric pulses (1–3 V).
- If the electric pulse intensity and duration as well as the electrode dimension remain constant, expanding the microchannel height reduces the number and radius of the large nanopores; the electroporated area of the cell membrane is also decreased.
- Increasing the electric pulse intensity intensifies the size and number of the created nanopores and increases the electroporated area on the cell membrane.
- Transmembrane potential becomes less widely spread for electrodes with a width larger than the cell diameter. The TMP profile is sinusoidal in the nonelectroporated area.
- If the width of the electrodes is smaller than the cell diameter, the local TMP decreases everywhere and sharply in the area from the poles (the nearest points of the cell membrane to the electrodes) to the equator.
- The number of created nanopores reaches its maximal value extremely fast; further presence of the electric pulse may not influence the number and location of the created nanopores anymore. It only develops the generated nanopores.
- Most nanopores are created around the poles.

Acknowledgments The authors acknowledge the financial support of the Canada Research Chair program and the Natural Sciences and Engineering Research Council of Canada through a research grant to D. Li.

References

Bao N, Le TT, Cheng J-X, Lu C (2010) Microfluidic electroporation of tumor and blood cells: observation of nucleus expansion and implications on selective analysis and purging of circulating tumor cells. Integr Biol (Camb) 2:113–120

Bilska AO, DeBruin KA, Krassowska W (2000) Theoretical modeling of the effects of shock duration, frequency, and strength on the degree of electroporation. Bioelectrochemistry 51:133–143

Cao Y, Yang J, Yin ZQ, Luo HY, Yang M, Hu N, Yang J, Huo DQ, Hou CJ, Jiang ZZ, Zhang RQ, Xu R, Zheng XL (2008) Study of high-throughput cell electrofusion in a microelectrode-array chip. Microfluid Nanofluid 5:669–675

DeBruin KA, Krassowska W (1999a) Modeling electroporation in a single cell. I. Effects of field strength and rest potential. Biophys J 77:1213–1224

DeBruin KA, Krassowska W (1999b) Modeling electroporation in a single cell. II. Effects of ionic concentrations. Biophys J 77: 1225–1233

Fox MB, Esveld DC, Valero A, Luttge R, Mastwijk HC, Bartels PV, van den Berg A, Boom RM (2006) Electroporation of cells in microfluidic devices: a review. Anal Bioanal Chem 385:474–485

Gimsa J (2001) A comprehensive approach to electro-orientation, electrodeformation, dielectrophoresis, and electrorotation of ellipsoidal particles and biological cells. Bioelectrochemistry 54:23–31

Gothelf A, Mir LM, Gehl J (2003) Electrochemotherapy: results of cancer treatment using enhanced delivery of bleomycin by electroporation. Cancer Treat Rev 23:371–387

Granot Y, Rubinsky B (2008) Mass transfer model for drug delivery in tissue cells with reversible electroporation. Int J Heat Mass Transf 51:5610–5616

Herwadkar A, Banga AK (2012) Peptide and protein transdermal drug delivery. Drug Discov Today Technol 9:e147–e154

Hibino M, Itoh H, Kinosita K (1993) Time courses of cell electroporation as revealed by submicrosecond imaging of transmembrane potential. Biophys J 64:1789–1800

Huang Y, Rubinsky B (2000) Micro-electroporation: improving the efficiency and understanding of electrical permeabilization of cells. Biomed Microdevices 3:145–150

Huang Y, Rubinsky B (2001) Microfabricated electroporation chip for single cell membrane permeabilization. Sens Actuators A Phys 89:242–249

Huang Y, Rubinsky B (2003) Flow-through micro-electroporation chip for high efficiency single-cell genetic manipulation. Sens Actuators A Phys 104:205–212

Ionescu-Zanetti C, Blatz A, Khine M (2008) Electrophoresis-assisted single-cell electroporation for efficient intracellular delivery. Biomed Microdevices 10:113–116

Jiang H et al (2011) A microfluidic chip for blood plasma separation using electro-osmotic flow control. J Micromech Microeng 21:085019

Khine M, Lau A, Ionescu-Zanetti C, Seo J, Lee LP (2005) A single cell electroporation chip. Lab Chip 5:38–43

Krassowska W, Filev PD (2007) Modeling electroporation in a single cell. Biophys J 92:404–417

Krassowska W, Neu JC (2009) Theory of electroporation. In: Efimov IR, Kroll MW, Tchou P (eds) Cardiac bioelectric therapy. Springer, New York

Lee WG, Demirci U, Khademhosseini A (2009) Microscale electroporation: challenges and perspectives for clinical applications. Integr Biol (Camb) 1:242–251

Li S (2008) Electroporation protocols: preclinical and clinical gene medicine. Springer, New York

Li J, Lin H (2011) Numerical simulation of molecular uptake via electroporation. Bioelectrochemistry 82:10–21

Lin Y-H, Leea G-B (2009) An optically induced cell lysis device using dielectrophoresis. Appl Phys Lett 94:033901

Miklavcic D, Towhidi L (2010) Numerical study of the electroporation pulse shape effect on molecular uptake of biological cells. Radiol Oncol 44:34–41

Movahed S, Li D (2011a) Electrokinetic transports through nanochannels. Electrophor J 32:1259–1267

Movahed S, Li D (2011b) Microfluidics cell electroporation. Microfluid Nanofluid 10:703–734

Movahed S, Li D (2012) Electrokinetic transport through the nanopores in cell membrane during electroporation. J Colloid Interface Sci 369:442–452

Neu JC, Krassowska W (1999) Asymptotic model of electroporation. Phys Rev E 59:3471–3482

Pauly H, Schwan HP (1959) Über die Impedanz einer Suspension von kugelförmigen Teilchen mit einer Schale. Z Naturforschung 14b: 125–131

Rafiei M, Mohebpour SR, Daneshmand F (2012) Small-scale effect on the vibration of non-uniform carbon nanotubes conveying fluid and embedded in viscoelastic medium. Physica E 44: 1372–1379

Schaper J, Bohnenkamp R, Noll H, Noll T (2007) New electrofusion devices for the improved generation of dendritic cell-tumour cell hybrids. In: Smith R (ed) Cell technology for cell products. Springer, New York

Shik Y, Cho SK, Kim JK, Lim SH, Park CH, Lee KB, Park Y, Chung C, Han D-C, Chang JK (2004) Electrotransfection of mammalian cells using a microchannel-type electroporation chip. Anal Chem 76:7045–7052

Talele S, Gaynor P, Cree MJ, van Ekeran J (2010) Modelling single cell electroporation with bipolar pulse parameters and dynamic pore radii. J Electrostat 68:261–274

Valero A, Post JN, van Nieuwkasteele JW, ter Braak PM, Kruijer W, van den Berg A (2008) Gene transfer and protein dynamics in stem cells using single cell electroporation in a microfluidic device. Lab Chip 8:62–67

Vassanelli S, Bandiera L, Borgo M, Cellere G, Santoni L, Bersani C, Salamon M, Zaccolo M, Lorenzelli L, Girardi S, Maschietto M, Dal Maschio M, Paccagnella A (2008) Space and time-resolved gene expression experiments on cultured mammalian cells by a single-cell electroporation microarray. New Biotechnol 25: 55–67

Wang H-Y, Lu C (2006a) Electroporation of mammalian cells in a microfluidic channel with geometric variation. Anal Chem 78:5158–5164

Wang H-Y, Lu C (2006b) High-throughput and real-time study of single cell electroporation using microfluidics: effects of medium osmolarity. Biotechnol Bioeng 95:1116–1125

Wang H-Y, Bhunia AK, Lu C (2006) A microfluidic flow-through device for high throughput electrical lysis of bacterial cells based on continuous dc voltage. Biosens Bioelectron 22:582–588

Wang S, Zhang X, Wang W, Lee LJ (2009) Semicontinuous flow electroporation chip for high-throughput transfection on mammalian cells. Anal Chem 81:4414–4421

Wang M, Orwar O, Olofsson J, Weber SG (2010) Single-cell electroporation. Anal Bioanal Chem 397:3235–3248

Weaver JC (1995) Electroporation theory: concepts and mechanisms. In: Nickoloff JA (ed) Plant cell electroporation and electrofusion protocols, vol 55., Humana PressTotowa, NJ, pp 3–28

Wong P, Tan W, Ho C-M (2005) Cell relaxation after electrodeformation: effect of latrunculin A on cytoskeletal actin. J Biomech 38:529–535

Yuejun K, Li D (2009) Electrokinetic motion of particles and cells in microchannels. Microfluid Nanofluid 6:431–460

Zaharoff DA, Henshaw JW, Mossop B, Yuan F (2008) Mechanistic analysis of electroporation-induced cellular uptake of macromolecules. Exp Biol Med (Maywood) 233:94–105

Zangle TA, Mani A, Santiago JG (2010) Theory and experiments of concentration polarization and ion focusing at microchannel and nanochannel interfaces. Chem Soc Rev 39:1014–1035

Zhao X, Zhang M, Yang R (2010) Control of pore radius regulation for electroporation-based drug delivery. Commun Nonlinear Sci Numer Simul 15:1400–1407

Zhengzheng F et al (2007) Gene transfection of mammalian cells using membrane sandwich electroporation. Anal Chem 79:5719–5722